ELSEVIER

www.elsevier.nl/locate/jorganchem

Journal of Organometallic Chemistry 613 (2000) 93–98

Journal of Organometallic Chemistry

Solid state ^{13}C-NMR and X-ray studies on the structure of tetraethylpyrazabole

Marek Dąbrowski [a], Janusz Serwatowski [a,*], Janusz Zachara [a], Anna Rufińska [b]

[a] *Faculty of Chemistry, Warsaw University of Technology (Politechnika), 00-664 Warsaw, Poland*
[b] *Max-Planck-Institut für Kohlenforschung, D-45470 Mülheim a.d. Ruhr, Germany*

Received 27 April 2000; received in revised form 16 July 2000

Abstract

DSC measurements of 4,4,8,8-tetraethylpyrazabole (**2**) show a high enthalpy phase transition in the solid state ($\Delta H = 28.61$ kJ mol^{-1}) at 69.0°C, far from its melting point at 106°C with $\Delta H = 3.22$ kJ mol^{-1}. ^{13}C-CP/MAS spectra of **2** show that at 69°C the ethyl groups attached to boron atoms start to rotate around the C–B bond and the whole molecule starts to rotate and to move changing its conformation from one boat to another. X-ray studies confirm its boat conformation in the solid state at room temperature.

Keywords: Tetraethylpyrazabole; Differential scanning calorimetry; Conformational study

1. Introduction

Although since its first synthesis in 1967 [1] a number of pyrazaboles were obtained and characterized, the conformation of the central six-membered B_2N_4 ring in molecule **1** and the influence of various factors on it are not fully understood (Scheme 1).

Since the last review in 1986 [2] only a few papers concerning the structure of pyrazaboles appeared in the literature [3–7]. Most pyrazaboles are well crystallized solids. They were found by X-ray analysis mainly in the boat conformation of the B_2N_4 ring. However, in a few cases they were also found in a chair and planar form but no electronic influence of the substituents at the boron or pyrazole (pz) framework in these conformations was found. It seems that the conformation of the pyrazabole B_2N_4 ring results mainly from the crystal packing effects. No other measurements in the solid state were performed. On the other hand, the recent applications of pyrazaboles as possible building blocks for discotic liquid crystals [8] or good bridges for *ansa*-ferrocenes to form the active container molecule [9–11] for supramolecular applications, encourage further studies on the structure of pyrazaboles, especially on the behavior of the B_2N_4 central ring and the factors influencing it in the solid state.

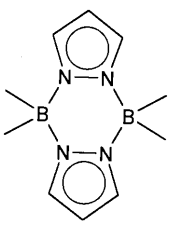

1

Scheme 1.

In our previous paper [12] we showed that 4,4,8,8-tetraethylpyrazabole (**2**) undergoes an unusual premelting endothermic phase transformation which was found by DSC and solubility measurements. These observations prompted us to investigate this phenomenon by solid state NMR measurements and optical observations as well as to find the crystal and molecular structure of this pyrazabole by X-ray diffraction.

2. Results and discussion

We have first tried to interpret the previously described premelting behavior of **2** (Scheme 2) (solid–

* Corresponding author. Fax: +48-22-6282741.
E-mail address: serwat@ch.pw.edu.pl (J. Serwatowski).

0022-328X/00/$ - see front matter
PII: S0022-328X(00)00507-6

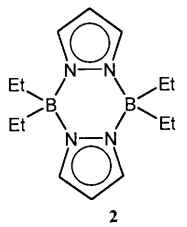

2

Scheme 2.

solid phase transition at 36 K below its melting point) as well as its behavior during dissolution [12] in terms of its dissociation to monomeric $Et_2B(pz)$ species, according to (Eq. (1)):

$$Et_2B(\text{-}pz)_2BEt_2 \leftrightarrows 2Et_2B(pz) \quad (1)$$

Although most pyrazaboles exist as stable dimers, it is possible that some of them could dissociate in solution at elevated temperature [10]. It was found that in the gas phase or in solution the derivatives with larger substituents on pyrazolyl rings could exist in a monomeric form even at room temperature [4]. To exclude possible dissociation the ^{11}B-NMR spectra were measured in the 20–80°C temperature range. No δ ^{11}B changes in these spectra proved that **2** exists as a dimer also above the transformation temperature.

Crystals of **2** viewed under polarized light through a microscope during the heating and melting determinations, showed to be optically anisotropic from room temperature to +68°C. At that temperature they lost refractivity and became optically isotropic, remaining crystalline without fusing or changing shape. Only at +106°C do they achieve m.p. The visual appearance of the crystalline **2** during heating, its behavior during solvation [12] as well as the large ratios of the premelting endothermic transition to the relatively small melting enthalpies (about 10:1) [12] are characteristic for plastic crystals. Phenomena observed in the plastic crystal may be well understood as a transition from an orientationally ordered state to an orientationally disordered state, that happens still in a solid state, where in the plastic-crystalline mesophase the molecules are undergoing rotational motion. We interpret the behavior

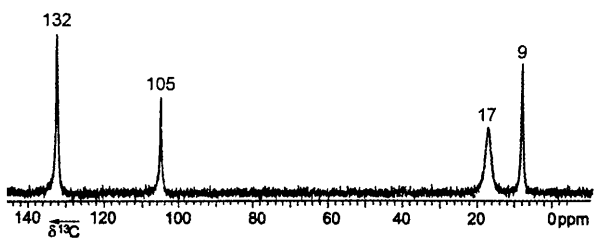

Fig. 1. ^{13}C-NMR spectra of solid **2** (m.p. 106°C) at 60 and 70°C.

of **2** at +68°C in terms of a transformation from crystal to plastic-crystalline phase.

Surprisingly, it was found that this transformation is unique for **2**. Other investigated pyrazaboles: the parent molecule $H_2B(pz)_2BH_2$ and $Pr_2B(pz)_2BPr_2$ showed only a melting transition. To explain this phenomenon solid state NMR measurements for **2** were performed.

Fig. 1 shows the ^{13}C-NMR spectra at 70°C for solidified **2**. At 70°C (2 K above the transition temperature) solid **2** gives four peaks ($\delta^{13}C = 135$, 107, 18, 10 ppm) corresponding to the pyrazole carbon atoms and ethyl group carbon atoms, respectively. A similar ^{13}C-NMR spectrum is obtained for the dissolved sample of **2** at room temperature. At 60°C no ^{13}C-NMR resonances for solid **2** are observed. This means that over 68°C the whole molecule starts to move, presumably to rotate, to enable the NMR observation. This confirms our interpretation of this phenomenon that at 68°C the sharp loss of optical anisotropy may be caused by the transformation to a higher symmetric cubic structure denoting a conversion to a plastic crystal state where molecular rotation occurs more easily.

We have also applied ^{13}C-CP/MAS-NMR spectroscopy, as this method has been used to study transitions between solid phases for typical five- and six-membered rings [13]. The corresponding spectrum of **2** at room temperature 297 K (Fig. 2a), shows contrary to the spectrum in solution a double signal set of equal intensities for the carbon atoms of the ethyl groups, while the signals of the pyrazolyl carbon atoms show the same appearance as in the solution. Typical spinning side bands (SSB) for carbon atoms are observed in the spectrum. At a higher temperature ($T =$ 353 K, 80°C) the spectrum becomes similar to that measured in solution. Only two signals for ethyl group carbon atoms are observed (Fig. 2c) compared to b). SSB remain in the spectrum. At higher temperatures (100°C, not shown) two signals of the ethyl group become narrower. After cooling to room temperature the spectrum shows the (a) appearance again.

Our observations indicate a reversible dynamic process, which occurs in **2** in the solid state. At room temperature compound **2** occurs in the boat conformation according to X-ray determinations. One can assume that at a higher temperature (above 68°C) ring inversion occurs (Scheme 3).

Both axial and equatorial ethyl groups became equivalent. At lower temperatures (room temperature) this inversion of the B_2N_4 ring is hindered and both ethyl groups became non equivalent.

Such a conformation change process for saturated and unsaturated five- and six-membered rings with the energy barrier of about 25 kJ mol^{-1} is known [14]. In our case the determined DSC enthalpy value of 28.61

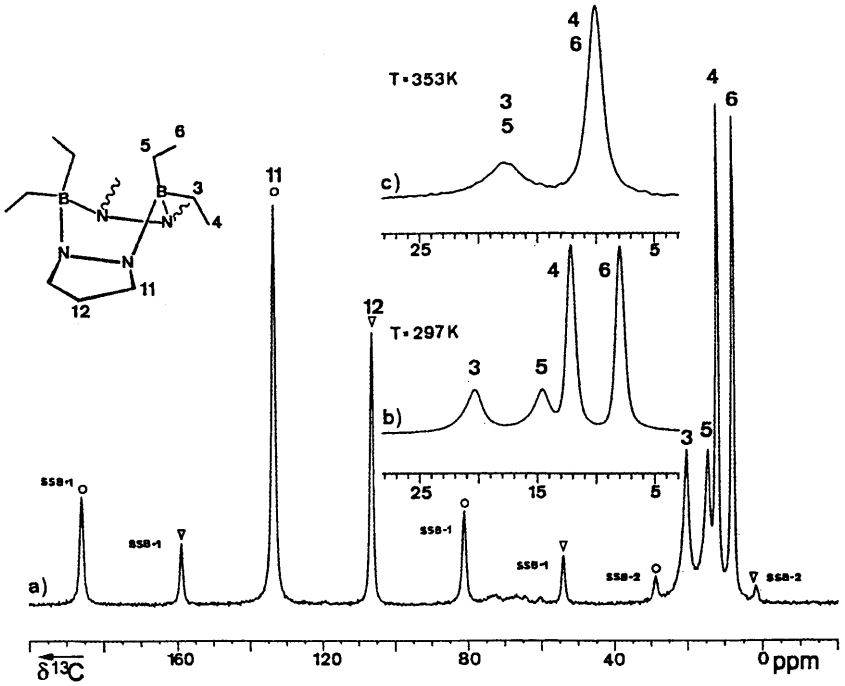

Fig. 2. Variable temperature 75.4 MHz ^{13}C-CP/MAS-NMR spectra of **2** (a, b) at $T = 297$ K; (c) at $T = 353$ K. The insets (b) and (c) show expansion of the aliphatic region of TOSS spectra. Spinning side bonds (SSB); $+n$ to higher frequency, $-n$ to lower frequency from isotropic chemical shift (denoted with number). SSB pattern for pyrazol — ^{11}C-atom was marked with O, for ^{12}C-atom with ▽. The same atom labeling as for X-ray analysis (Fig. 3) was used in ^{13}C-CP/MAS spectra.

kJ mol^{-1} for the phase transition fits well to this data. Furthermore, both the ^{13}C spectrum of the solidified sample as well as the ^{13}C-CP/MAS-NMR measurements indicate that there are two different types of motion: overall molecular rotation and internal rotation of the ethyl groups around B–C bonds which forces the ring inversion. We believe that our transition from the crystal to plastic phase for **2** at 68°C can be interpreted in terms of these two types of motions.

Fig. 3a,b shows the results of the X-ray structure analysis of crystalline **2** obtained at room temperature. The compound crystallizes in the monoclinic system space group $P2_1/m$ with two molecules in the unit-cell. In Table 1 some selected bond lengths and angles are listed. In general they are close to those observed for other tetraalkylpyrazaboles. **2** posses a C_s point symmetry with the symmetry plane perpendicular to the B(1)···B(1′) axis. Both C(12) and C(22) atoms belong to this plane. The boron atoms are tetracoordinated, which is confirmed by almost an ideal sp^3-hybrydization sphere around them. The B(1)–C(3) and B(1)–C(5) bonds as well as B(1)–N(1) and B(1)–N(2) bonds are almost identical, respectively. The central B_2N_4 ring has the boat conformation with four nitrogen atoms in the plane and boron atoms located 0.262(2) Å over this plane. The corresponding N_4-plane/BN_2-plane dihedral angle equals 15.9(1)°. Neither pyrazolyl plane is coplanar. Fig. 3b shows, however that each pyrazolyl plane is almost coplanar with the BNNB plane forming two

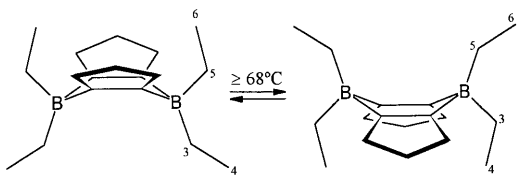

Scheme 3.

Table 1
Selected bond lengths and angles for **2** [a]

Bond lengths (Å)			
N(1)–C(11)	1.338(2)	N(2)–C(21)	1.336(2)
N(1)–N(1′)	1.345(2)	N(2)–N(2′)	1.348(2)
N(1)–B(1)	1.573(2)	N(2)–B(1)	1.578(2)
B(1)–C(3)	1.607(2)	B(1)–C(5)	1.609(2)
C(3)–C(4)	1.514(3)	C(5)–C(6)	1.513(2)
C(11)–C(12)	1.354(2)	C(21)–C(22)	1.358(2)
Bond angles (°)			
C(11)–N(1)–N(1′)	107.50(10)	C(21)–N(2)–N(2)	107.55(9)
N(1′)–N(1)–B(1)	125.81(7)	N(2′)–N(2)–B(1)	125.63(7)
N(1)–B(1)–N(2)	105.24(11)	C(3)–B(1)–C(5)	115.08(13)
N(1)–B(1)–C(3)	108.49(13)	N(2)–B(1)–C(3)	108.54(13)
N(1)–B(1)–C(5)	108.35(12)	N(2)–B(1)–C(5)	110.66(12)
N(1)–C(11)–C(12)	110.0(2)	N(2)–C(21)–C(22)	110.0(2)
C(11′)–C(12)–C(11)	105.1(2)	C(21′)–C(22)–C(21)	105.0(2)

[a] Symmetry transformations used to generate equivalent atoms (designated by prime): x, $-y+1/2$, z.

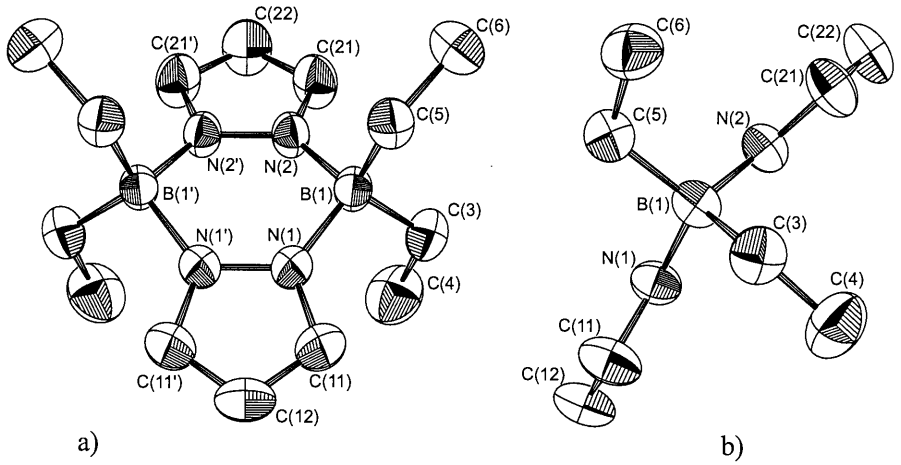

Fig. 3. ORTEP diagram of **2** with 50% probability thermal ellipsoids.

planes, which form a dihedral angle of 19.9(1)°. Both pyrazolyl ligands are symmetrical to the plane containing both boron atoms and all methylene group carbon atoms. Both methyl group carbon C(4) and C(4′) atoms also lie in this plane. Surprisingly both C(6) and C(6′) atoms are located out of this plane (quasi-C_{2v} point group symmetry of the whole molecule, except C(6) and C(6′) atoms).

The crystal structure of **2** at higher temperatures was also investigated by X-ray powder diffraction. At 80°C only three lines were observed in the powder patterns indicating the transformation to the form which has the higher crystal symmetry. The rapid decrease in intensity with increasing Bragg angle is explained by rotational disorder, which approaches the spherical symmetry. For three observed reflections 110, 200 and 211 it was deduced that the structure is a body-centered cubic with two molecules in the unit cell. The calculated unit cell parameters $a = 9.782$ Å, $V = 936$ Å^3, volume per non-hydrogen atom 23.4 Å^3 is consistent with those obtained in the single-crystal measurements.

3. Conclusions

(a) A solid-solid phase transition was found for **2** at 68°C, below its m.p. at 106°C. (b) This transition can be assumed as a crystal to plastic crystal transformation. (c) The nature of this transformation is not only a typical rapid in-place motion (rotation) of molecules in the plastic form. We believe that additional internal rotation of the ethyl groups around the B–C bond occurs in the molecule. (d) This internal rotation also forces a B_2N_4 ring inversion from one boat to another, causing an axial–equatorial change of the ethyl groups, with a butterfly-like movement of the pyrazolyl ligands.

4. Experimental

Pyrazabole, 4,4,8,8-tetraethylpyrazabole and 4,4,8,8-tetrapropylpyrazabole were received from the Department of Chemistry, University of Kentucky, Lexington, KY, USA. Visual observations were performed on a BIOLAR PI microscope.

4.1. NMR measurements

Variable temperature ^{11}B-NMR spectra were run on a Unity Plus 200 MHz spectrometer in a C_6D_6 solution ($Et_2O{\cdot}BF_3$ external standard) in the temperature range of 20–80°C. The only ^{11}B-NMR signal was observed in the spectra at $\delta\ ^{11}B = 3.7$ ppm.

^{13}C-NMR spectra were run on a Gemini 200 MHz instrument. Samples were first melted and then solidified in a special 3-mm tube. This tube was then inserted into another ordinary 5-mm NMR tube, which contained DMSO with TMS. The spectrum at 70°C (liquid-like spectrum) showed four signals at 135, 107, 18 (broad) and 10 ppm, respectively.

Solid state ^{13}C-CP/MAS-NMR spectra were measured on a Bruker MSL-300 spectrometer equipped with a CP/MAS double bearing probe and a Bruker BV-100 temperature control unit. ZrO_2 rotors (7 mm o.d.) were spun at spin rates ~ 4 kHz. Adamantane was used as an external standard $\delta_{TMS}(CH_2) = 38.40$. Typical 90° pulses are ca. 4 μs for ^{1}H, and 4.3 μs for ^{13}C, respectively, with an optimized contact time at 3 ms.

^{13}C-CP/MAS (75.4 MHz). $T = 297$ K, $\delta = 8.0$ (C6), 12.2 (C4), 14.6 (C5), 20.6 (C3), 106.5 (C12), 133.5 (C11). $T = 353$ K, $\delta = 10.0$ (C4 + C6), 17.8 (C3 + C5), 106.6 (C12), 133.7 (C11). Assignments of all the signals according to [15].

Table 2
Crystal data and structure refinement for **2**

Empirical formula	$C_{14}H_{26}B_2N_4$
Formula weight	272.01
Temperature (K)	293(2)
Wavelength (Å)	0.71073 (Mo–K_α)
Crystal system	Monoclinic
Space group	$P2_1/m$
Unit cell dimensions	
a (Å)	7.3135(10)
b (Å)	15.992(3)
c (Å)	7.4977(11)
β (°)	111.443(12)
V (Å^3)	816.2(2)
Z	2
D_{calc} (g cm^{-3})	1.107
Absorption coefficient (mm^{-1})	0.062
Crystal size (mm)	$0.30 \times 0.24 \times 0.20$
θ Range for data collection (°)	2.55–25.05
Index ranges:	$0 \le h \le 8,\ 0 \le k \le 18,\ -8 \le l \le 8$
Reflections collected	1619
Independent reflections	1499 ($R_{int} = 0.0172$)
Refinement method	Full-matrix least-squares on F^2
Data/restraints/parameters	1499/0/149
Goodness of fit on F^2	1.018
Final R indices [$I > 2\sigma(I)$]	$R_1 = 0.0389,\ wR_2 = 0.1001$
R indices for all data	$R_1 = 0.0552,\ wR_2 = 0.1102$
Extinction coefficient	0.024(5)
Largest difference peak/hole (e Å^{-3})	+0.16/−0.17

Table 3
Atomic coordinates ($\times 10^4$) and equivalent isotropic displacement parameters (Å$^2 \times 10^3$) for **2**

Atom	x	y	z	U_{eq} [a]
N(1)	1775(2)	2921(1)	6968(2)	46(1)
N(2)	3951(2)	2921(1)	5052(2)	45(1)
B(1)	2550(2)	3496(1)	5696(2)	44(1)
C(3)	3835(3)	4236(1)	7015(3)	58(1)
C(4)	5509(4)	3970(2)	8813(3)	84(1)
C(5)	699(2)	3798(1)	3868(2)	52(1)
C(6)	1128(3)	4417(1)	2544(3)	68(1)
C(11)	902(3)	3172(1)	8163(3)	64(1)
C(12)	341(4)	2500	8937(4)	70(1)
C(21)	5283(3)	3173(1)	4334(3)	61(1)
C(22)	6139(4)	2500	3856(4)	67(1)

[a] U_{eq} is defined as one third of the trace of the orthogonalized U_{ij} tensor.

4.2. X-ray crystallographic analysis of **2**

Crystals suitable for X-ray analysis were recrystallized from ethanol and then crystallized by vacuum sublimation. Diffraction data was measured for a single crystal at 293 K with graphite–monochromated Mo–K_α radiation on the Siemens P3 four-circle diffractometer. The unit-cell parameters were obtained from the least-squares refinement of the setting angles of 21 reflection ($7.9 \le \theta \le 12.3°$). Intensities were measured in θ–2θ scan mode with a variable scan speed within a range $5.0 \le 2\theta \le 50.0°$). Two check reflections measured every 70 reflections, indicated appreciable (21.2%) decomposition of the crystal during data collection. Appropriate correction for decay was applied. The structure was solved by direct methods using SHELXS-86 program [16] and was refined using the full-matrix least-squares technique on F^2 (SHELXL-93) [17]. Anisotropic temperature factors were used for all non-hydrogen atoms. The isotropic displacement parameters and positional parameters of all H atoms were refined without constrain. An isotropic extinction coefficient χ was refined to a value 0.024(5). The final weighting scheme was $w = [\sigma^2(F_o^2) + (0.0549P)^2 + 0.1309P]^{-1}$ where $P = (F_o^2 + 2F_c^2)/3$. The largest positive and negative peaks on a last difference Fourier synthesis (+0.16/−0.17 e Å^{-3}) have no significant chemical meaning. Maximum shift/error in the final cycles of refinement was < 0.001. Remaining crystallographic data and atom coordinates are listed in Tables 2 and 3, respectively.

4.3. X-ray powder diffraction analysis of **2**

The sample was obtained by sublimation and was sealed in an aluminum can of ~ 10 mm diameter. X-ray powder diffraction data at room temperature and 80°C were collected on a DRON 2.0 diffractometer equiped with a UWD 2000 high temperature camera with Cu–K_α radiation ($\lambda = 1.542$ Å). The lattice parameters were calculated from three reflections with $5.0° \le 2\theta \le 40°$.

5. Supplementary material

Crystallographic data for the structural analysis has been deposited with the Cambridge Crystallographic Data Center, CCDC No. 142387 for compound **2**. Copies of this information may be obtained free of charge from: The Director, CCDC, 12 Union Road, Cambridge, CB2 1EZ UK (Fax: +44-1223-336033; e-mail: deposit@ccdc.cam.ac.uk or www: http://www.ccdc.cam.ac.uk

Acknowledgements

The authors thank Professor Kurt Niedenzu (University of Kentucky) for pyrazaboles used in this work and Professor Adam Gryff-Keller (Warsaw University of Technology) for helpful discussion.

References

[1] S. Trofimenko, J. Am. Chem. Soc. 89 (1967) 3165.
[2] K. Niedenzu, S. Trofimenko, Top. Curr. Chem. 131 (1986) 1.
[3] J. Bielawski, M.K. Das, E. Hanecker, K. Niedenzu, H. Nöth, Inorg. Chem. 25 (1986) 4623.
[4] M. Yalpani, R. Boese, R. Köster, Chem. Ber. 123 (1990) 1275.
[5] T.G. Hodkins, D.R. Powell, Acta Crystallogr. Sect. C C48 (1992) 1260.
[6] V.O. Atwood, D.A. Atwood, A.H. Cowley, S. Trofimenko, Polyhedron 11 (1992) 711.
[7] C.M. Clarke, M.K. Das, E. Hanecker, J.F. Mariategui, K. Niedenzu, P. Niedenzu, H. Nöth, K.R. Warner, Inorg. Chem. 26 (1987) 2310.
[8] J. Barberá, R. Giménez, J.L. Serrano, Adv. Mat. 6 (1994) 470.
[9] F. Jäkle, T. Priermeier, M. Wagner, Organometallics 15 (1996) 2033.
[10] E. Herdtweck, F. Jäkle, G. Opromolla, M. Spigler, M. Wagner, P. Zanello, Organometallics 15 (1996) 5524.
[11] F. Jäkle, F. Peters, T. Priermeier, M. Wagner, Abstracts of IMEBORON-IX, University of Heidelberg, Heidelberg, Germany, July, 1996.
[12] U. Domanska, J. Serwatowski, A. Sporzynski, M. Dabrowski, Thermochim. Acta 222 (1993) 279.
[13] J.B. Lambert, S.C. Jonnson, L. Xue, J. Am. Chem. Soc. 116 (1994) 6167.
[14] H. Günther, NMR Spektroskopie, Verlag, Stüttgart, 1983, p. 241.
[15] H.O. Kalinowski, S. Berger, S. Braun, ^{13}C-NMR-Spektroskopie, Verlag, Stüttgart, 1984, p. 103.
[16] G.M. Sheldrick, Acta Crystallogr. Sect. A 46 (1990) 467.
[17] G.M. Sheldrick, SHELXL-93: Program for the Refinement of Crystal Structures, University of Göttingen, Germany, 1993.